

THE 4TH INTERNATIONAL CONFERENCE ON ALUMINUM ALLOYS

MICROSTRUCTURAL EVOLUTION DURING SUPERPLASTIC DEFORMATION OF 2095 Al-Li ALLOY

P. Kitabjian; Dept. of Material Science, Stanford University, Stanford, CA 94305
E. W. Lee; Code 6063, Naval Air Warfare Center, A/C Div., Warminster, PA 18974

Introduction

Al-Li alloys offer extremely attractive combinations of properties to designers of high-performance military and commercial aircraft. The advantages of Al-Li alloys compared to conventional high strength alloys are low density, high strength and modulus, good low temperature capabilities and resistance to fatigue crack propagation. Superplastic forming (SPF) in conjunction with the light weight of Al-Li alloys may contribute to a significant further weight saving for aircraft structure. Also the reduction in the number of fabrication processes by SPF significantly reduces total cost of airframe construction. However, the problems associated with various properties rather than processing such as anisotropy, T8 requirement, poor stress corrosion resistance, reduced strength due to recrystallization and difficulties involved in resolution, quenching and reaging, have been the obstacles for the full implementation of SPF Al-Li alloys to advanced aircraft.

The Al-Li alloy 2095 was originally designated as the Weldalite 049 which was developed by the Martin Marietta. The superplastic grade of the 2095 is now being produced by Reynolds Metals Co. The alloy exhibits very high strength and an excellent stress corrosion cracking resistance. Also the alloy shows considerably less anisotropy and respectable post-SPF mechanical properties. Recent NAWC Warminster study shows that the 2095 alloy is superplastic in wide range of strain rates and temperatures. The primary purpose of this study was to define superplastic characteristic of alloy 2095 and optimize temperatures and strain rates for maximum elongation and minimum cavitation. This paper will describes all the superplastic parameters and microstructural change associated with varying superplastic temperatures and strain rates.

Experimental Procedure

The superplastic grade aluminum alloy 2095 used in this experiment has the nominal chemical composition of 4.75% Cu, 1.30% Li, 0.40% Mg, 0.40% Ag and 0.14% Zr (Wt.%). Material was obtained from Reynolds Metals Co. in sheet form. This alloy underwent thermomechanical treatments resulting in an unrecrystallized material with very fine grain structure. The microstructure of the as-received material is shown in figure 1.

Tensile specimens were machined from the as-received sheet to the following dimensions : 0.33 in. gage length, 0.25 in. width, with a 0.092 in. sheet thickness. A typical specimen is shown in figure 2. The tensile axis of each specimen was aligned with the sheet rolling direction.

Tension testing was performed using an 20,000 pound Instron equipped with a three-zone furnace and chromel-alumel thermocouples to control and monitor the test temperature. The temperatures investigated ranged from 480°C to 535°C, and were controlled to within +/-2°C during testing. The cross-head speed was constant during testing, and initial strain rates investigated ranged from $5.0 \times 10^{-4} \text{ sec}^{-1}$ to $1.0 \times 10^{-2} \text{ sec}^{-1}$. The true strain rates decreased during testing as the specimens elongated.

Optical micrography of the specimens was performed using a Nikon Epiphot - TME. For each specimen examined, a section normal to the tensile direction was taken 5 mm from the fracture surface. The extent of cavitation of fractured specimens was determined using a Cambridge Quantimet 970 image analysis system. The mean grain size was determined visually at 400x, using the line intercept method.

The strain rate sensitivity of the material was determined at each test temperature by stepping the strain rate incrementally from a small baseline value of $2.5 \times 10^{-4} \text{ sec}^{-1}$ through eight higher strain rates, up to 0.1 sec^{-1} . The test duration, after allowing the specimen to stabilize at the test temperature, was less than 5 minutes. The strain rate sensitivity, m , was determined by measuring the change in stress associated with each change in strain rate :

$$m = \Delta \log(\text{stress}) / \Delta \log(\text{strain rate}).$$

The log stress - log strain rate curve was expected to vary sigmoidally; the m value was determined from the linear region of the curve (strain rate between 0.001 and 0.01 sec^{-1}), where the slope was a maximum.

Results

The material was found to have maximum ductility at 490°C at an initial strain rate of approximately $2.5 \times 10^{-3} \text{ sec}^{-1}$, as seen in figure 3. A 1300% elongation was achieved under these conditions (figure 2). Ductility approximately doubled when the test temperature was increased from 480°C to 490°C, then decreased gradually as the test temperature was further increased. At 525°C, an elongation greater than 700% could not be achieved.

At most of the test temperatures, the ductility of the material improved with increasing strain rate, reaching a maximum at an initial strain rate of $5.0 \times 10^{-3} \text{ sec}^{-1}$. Initial strain rates higher than $5.0 \times 10^{-3} \text{ sec}^{-1}$ resulted in poorer ductility. Elongations greater than 800% could not be achieved at 0.01 sec^{-1} initial strain rate.

The stress--strain curves for these specimens in tension were similar in shape. The stress would increase linearly until yielding, and would further increase to some peak value, still during the early stages of testing. Then, as the cross-sectional area of the sample was reduced, the flow stress would decrease gradually, approaching zero. Typically greater than 95% of the time of testing was spent plastically elongating the specimen. The test duration, after approximately 30 minutes to stabilize at the test temperature, ranged from 10 minutes to 6 hours.

The peak stress varied approximately linearly with the logarithm of the strain rate and could be minimized by reducing the strain rate (figure 4). A peak stress as low as 280 psi was achieved at an initial strain rate of 10^{-3} sec^{-1} and temperature of 515°C. In general, the peak stress decreased with increasing temperature.

The strain rate sensitivity coefficient, m , varied with temperature as shown in figure 5. The m value ranged from about 0.5 between 480°C and 500°C, rising to 0.62 at 525°C. The strain rate spiking procedure yielded sigmoidal log stress versus log strain rate relations as expected,

with linear regions between the strain rate range 0.001 and 0.01 sec^{-1} (figure 6). It is evident from this figure that a given strain rate generated higher stress at lower temperatures than at higher temperatures.

The grain sizes, as measured by the mean intercept length, ranged from 3.2×10^{-4} to 5.6×10^{-4} inches. The photomicrographs in figure 7 show the increase in grain size with decreasing strain rate. The recrystallized grain size did not show a strong temperature dependence. The photomicrographs in figure 8 show little variation in grain size as the temperature increases. Tests performed at higher strain rates, where the test duration was shorter, resulted in smaller grain sizes.

Straining of the specimens caused intergranular cavitation, as shown in figure 9. These voids may have ultimately led to failure. The extent of cavitation was determined for several of the specimens. There does not appear to be a strong dependence on the strain rate. However, a temperature dependence of cavitation is obvious. The extent of cavitation increases with temperature.

Discussion

Optimization of elongation with respect to strain rate and temperature involves the consideration of grain boundary sliding mobility and grain growth. In the temperature range investigated, the primary deformation mechanism is grain boundary sliding. To accommodate this mechanism, a fine recrystallized grain structure is required. High temperatures can result in grain coarsening during elongation, thereby reducing the material's ability to deform. This phenomenon limits the elongations achieved at higher temperatures as seen in figure 3. Test temperatures of 480°C resulted in much lower elongations than observed for the same strain rate at 490°C . At low temperatures, the grain boundary sliding accommodated by diffusion is not fully operational, therefore ductility is limited. These two competing processes result in a maximum ductility between 490°C and 500°C .

Figure 3 shows that increasing the strain rate results in greater ductility, provided that the strain rate is not too high to be accommodated by a stable deformation mechanism. A very high strain rate (0.01 sec^{-1}) may not allow the material enough time to flow plastically. At low strain rates ($5 \times 10^{-4} \text{ sec}^{-1}$), the time required to produce high elongations is great (4-8 hours). Grain growth can therefore proceed to a greater degree, and thereby reduce the material's ability to deform by grain boundary sliding. Evidence for this behavior is found in figure 7 which shows that higher strain rates result in smaller grains. An initial strain rate of $5 \times 10^{-3} \text{ sec}^{-1}$ produces maximum elongation at most of the test temperatures.

As mentioned previously, the peak stress for this tension test is reached during the early stages of testing, when grain growth may have not yet occurred to a great degree. The anomalous increase in peak stress for the initial strain rate of 0.001 sec^{-1} from 515°C to 525°C may be due to grain growth; at this low strain rate and relatively high temperature there may have been enough time for coarsening to occur even before the peak stress was reached.

Figure 4 shows that higher strain rates result in higher peak stresses. This behavior is due to the strain rate sensitivity of the material, which has been shown to equal approximately 0.5 to 0.6 in the temperature range investigated. This effect is also seen in figure 6, where higher strain rates result in higher flow stresses. A given strain rate generates higher stress at lower temperatures than at higher temperatures. This is due to the higher mobility of the grains at higher temperatures. The short duration of the test minimizes the effects of grain growth which can influence this behavior at higher temperatures.

The strain rate sensitivity coefficient (m) increases with increasing temperature, as shown in figure 5. A high m value usually corresponds to high ductility; this does not agree, however with the observed behavior. This material exhibits maximum elongation at 490°C and 500°C, but has a maximum m value at 525°C. A possible explanation of this behavior is that the effects of grain coarsening and cavitation are not exhibited in the m value testing due to the short duration of this test. The results indicate that this material might actually have greater ductility at 525°C if the effects of grain coarsening and increased cavitation could be inhibited. The recrystallized grain size of this material is dependent on the extent of grain growth which has occurred. This process requires sufficient thermal energy and time. Figure 7 indicates that high strain rates result in smaller grain sizes. The time required to elongate a specimen at a high strain rate can be 20 times less than is necessary at a low strain rate, thus less grain growth has occurred at the higher strain rates. It is also expected that higher temperatures will result in larger grain sizes, however, this is not the case in figure 8. It should be considered that the duration of each test may have varied greatly. One possible conclusion that may be drawn from this is that grain growth is a stronger function of the duration of the test rather than the temperature.

Cavitation during elongation often leads to the ultimate failure of a specimen. The extent of cavitation is an important characteristic to consider when optimizing processing conditions. One might expect that higher strain rates would lead to greater cavitation, as the microstructure has less time to rearrange during deformation. The larger grain size which accompanies the slower strain rates, however, may contribute to larger void formation and nullify any positive effect slow deformation may have had. Figure 9 shows that there is no clear strain rate dependence of cavitation. However, larger size cavities are observed at slower strain rate deformation and vice versa. Also it is notified that larger cavities are more likely found with larger grain size deformation microstructure. Large grains can not exhibit grain boundary sliding as easily as small grains, thus deformation can not occur as easily and voids are more likely to form.

Conclusions

1. The Al-Li alloy 2095 exhibited 1300% elongation at 490°C at the initial strain rate of $2.5 \times 10^{-3}/\text{sec}$.
2. The alloy 2095 showed superplastic elongation (more than 500%) in the wide range of temperature (480°C-525°C) and strain rate ($5 \times 10^{-4}/\text{sec}$ - $5 \times 10^{-3}/\text{sec}$).
3. In general, the superplastic elongation increased with increasing strain rate in the strain rate range from $5 \times 10^{-3}/\text{sec}$ to $5 \times 10^{-4}/\text{sec}$. This is associated with decreasing recrystallized grain size with increasing strain rate.
4. There was no clear strain rate dependency of cavitation. This is due to the two competing mechanisms. The decreasing grain size with increasing strain rate suppresses the formation of cavity. However, the formation of cavity is enhanced by the less available diffusion time with increasing strain rate.

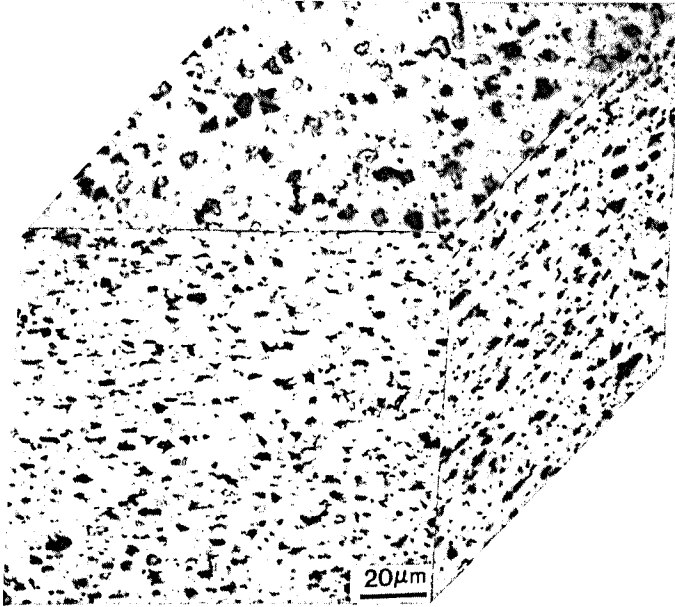


Figure 1- Microstructure of as-received aluminum 2095 alloy

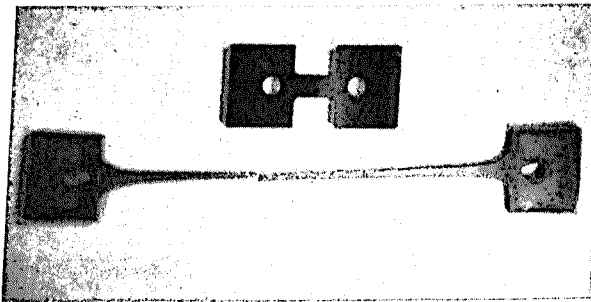


Figure 2 - Top - undeformed superplastic tensile specimen. Bottom - tensile specimen after elongation to 1300%

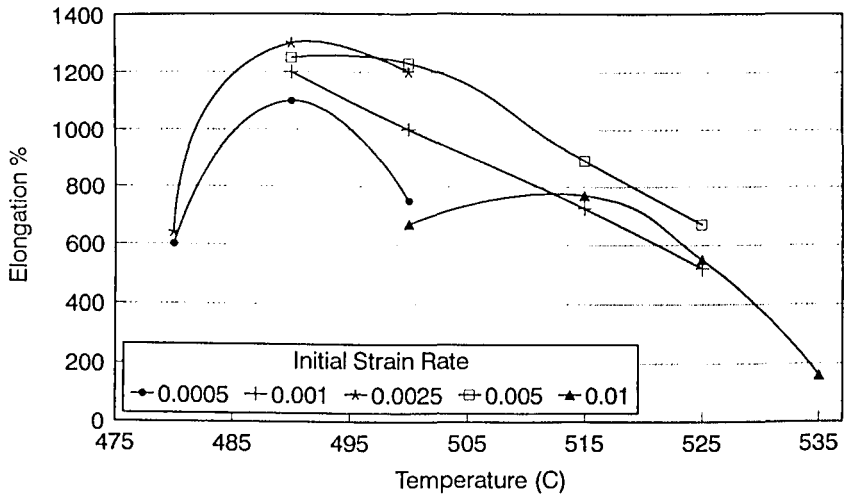


Figure 3 - Superplastic elongation of 2095 Al-Li alloy vs. temperature at various strain rates.

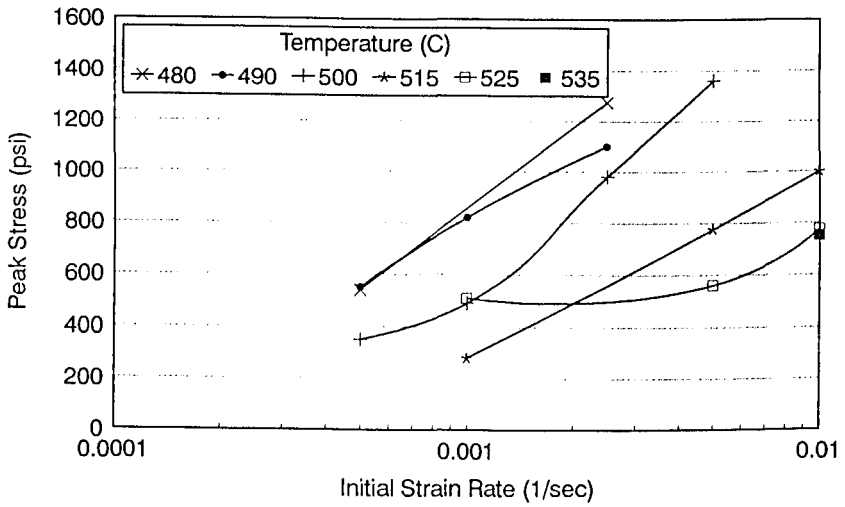


Figure 4 - Peak stress vs. strain rate at various temperatures.

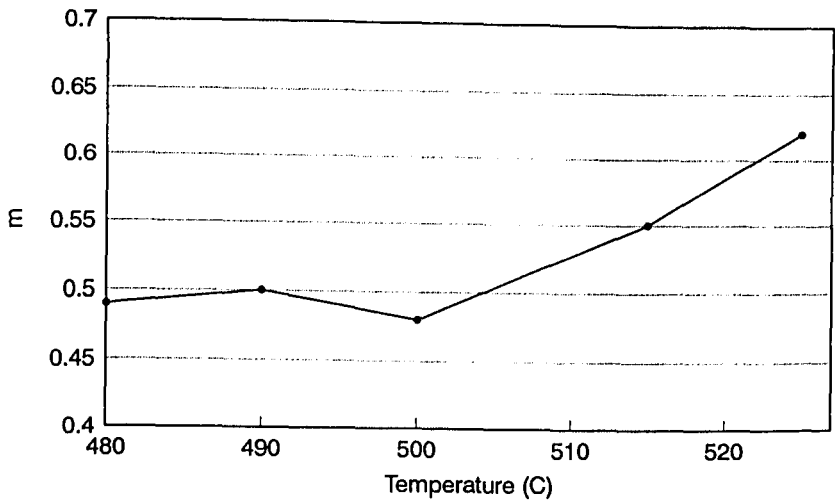


Figure 5 - Variation of strain rate sensitivity coefficient, m, as a function of temperature.

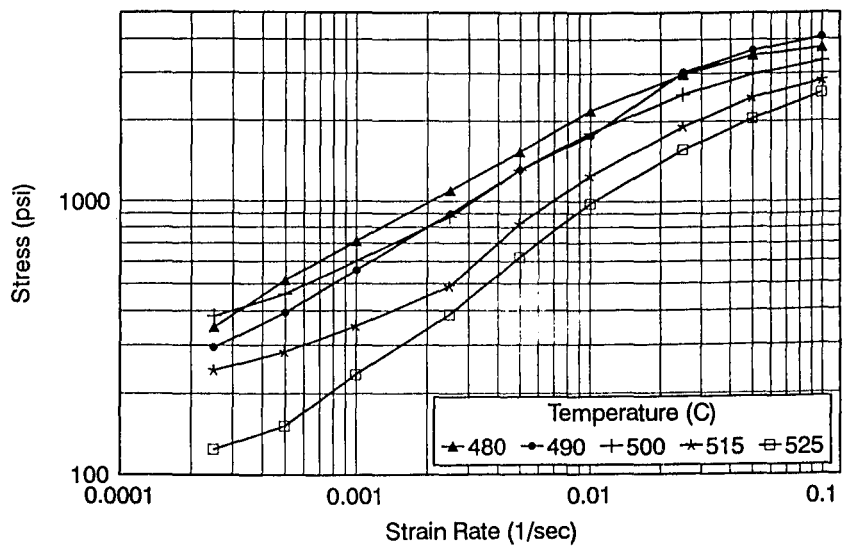


Figure 6 - Stress vs. strain rate at various temperatures showing sigmoidal curves.

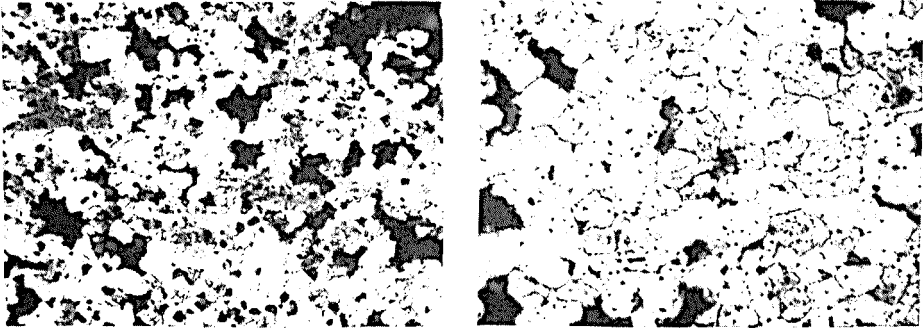


Figure 7 - Optical micrographs showing decreasing grain size with increasing strain rate at 500°C, strain rate: $10^{-2}/\text{sec}$ (left), $10^{-3}/\text{sec}$ (right)

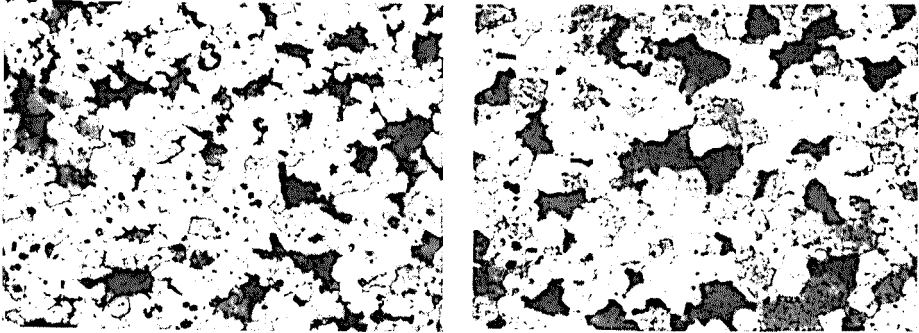


Figure 8 - Optical micrographs showing grain structure deformed at 495°C(left) and 515°C(right)

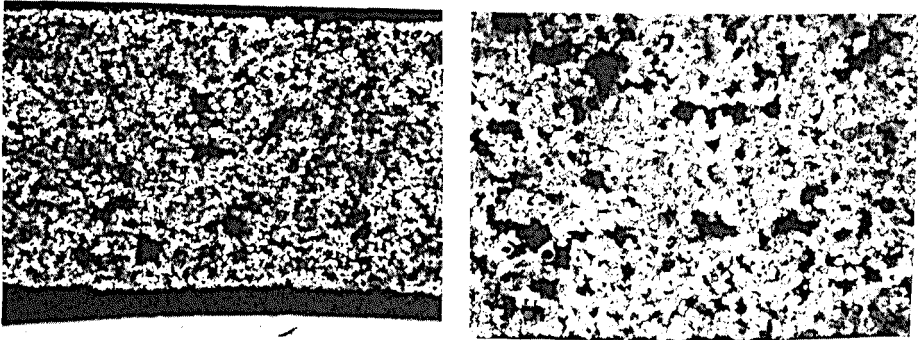


Figure 9 - Cavitation near fracture surface at 500°C, strain rate: $10^{-2}/\text{sec}$ (left), $10^{-3}/\text{sec}$ (right)